# NASA Technical Memorandum

NASA TM - 103536

# EFFECT OF FLANGE BOLT PRELOAD ON SPACE SHUTTLE MAIN ENGINE HIGH PRESSURE OXIDIZER TURBOPUMP HOUSING ANALYSIS

By J.B. Min, L.M. Johnston, and B. Czekalski

Structures and Dynamics Laboratory
Science and Engineering Directorate

May 1991



National Aeronautics and Space Administration

George C. Marshall Space Flight Center

NASA
National Aeronautics and Space Administration

# Report Documentation Page

| 1. Report No. | 2. Government Accession No. | 3. Recipient's Catalog No. |
|---|---|---|
| NASA TM-103536 | | |

| 4. Title and Subtitle | 5. Report Date |
|---|---|
| Effect of Flange Bolt Preload on Space Shuttle Main Engine High Pressure Oxidizer Turbopump Housing Analysis | May 1991 |
| | 6. Performing Organization Code |

| 7. Author(s) | 8. Performing Organization Report No. |
|---|---|
| J.B. Min, L.M. Johnston, and B. Czekalski* | 10. Work Unit No. |

| 9. Performing Organization Name and Address | 11. Contract or Grant No. |
|---|---|
| George C. Marshall Space Flight Center<br>Marshall Space Flight Center, Alabama 35812 | 13. Type of Report and Period Covered<br>Technical Memorandum |

| 12. Sponsoring Agency Name and Address | 14. Sponsoring Agency Code |
|---|---|
| National Aeronautics and Space Administration<br>Washington, DC 20546 | |

15. Supplementary Notes

Prepared by Structures and Dynamics Laboratory, Science and Engineering Directorate.

*Intergraph Corporation

16. Abstract

Cracks at the seal fillet flange and the strut pilot groove of primary turbine drain passage of the space shuttle main engine (SSME) high pressure oxidizer turbopump (HPOTP) have been observed and reported. Stress information for critical structural components in the SSME under actual conditions is necessary for design and life prediction analysis. However, little information is available about the stress distribution at this location under various combinations of loadings and environments. Thus, a stress analysis was conducted to determine an influence of the various operation and installation loads on the stresses of the HPOTP main mounting flange. To do this, a three-dimensional (3-D) finite element model of the HPOTP housing was generated. A fairly comfortable margin of stresses at the flange fillet with respect to the yield stress of Inconel 718 is shown in this analysis. However, it was revealed that the bending stress arising from the housing flange bolt preloads could significantly affect the stress distribution at the strut pilot groove of primary turbine drain passage in the HPOTP housing. Consequently, the information obtained from the present 3-D analysis results should be useful in guiding the development of the SSME HPOTP.

| 17. Key Words (Suggested by Author(s)) | 18. Distribution Statement |
|---|---|
| HPOTP flange bolt preload,<br>space shuttle main engine, cracks,<br>3-D finite elements HPOTP model,<br>fracture mechanics | Unclassified - Unlimited |

| 19. Security Classif. (of this report) | 20. Security Classif. (of this page) | 21. No. of pages | 22. Price |
|---|---|---|---|
| Unclassified | Unclassified | 36 | NTIS |



For sale by the National Technical Information Service, Springfield, VA 22161-2171

## ACKNOWLEDGMENT

The authors acknowledge useful discussions with Lee Awad of the Rocketdyne Division of Rockwell International and Greg Sisk of Lockheed Missiles & Space Company.

## TABLE OF CONTENTS

## LIST OF FIGURES

## LIST OF ILLUSTRATIONS (Continued)

## LIST OF TABLES

TECHNICAL MEMORANDUM

# EFFECT OF FLANGE BOLT PRELOAD ON SPACE SHUTTLE MAIN ENGINE HIGH PRESSURE OXIDIZER TURBOPUMP HOUSING ANALYSIS

## SUMMARY

Cracks at the seal fillet flange and the strut pilot groove of primary turbine drain passage of the space shuttle main engine (SSME) high pressure oxidizer turbopump (HPOTP) have been observed and reported. Stress information for critical structural components in the SSME under actual conditions is necessary for design and life prediction analysis. However, little information is available about the stress distribution at this location under various combinations of loadings and environments. Thus, a stress analysis was conducted to determine the influence of the various operation and installation loads in the stresses of the HPOTP main mounting flange. To do this, a three-dimensional (3-D) finite element model of the HPOTP housing was generated. A fairly comfortable margin of stresses at the flange fillet with respect to the yield stress of Inconel 718 is shown in this analysis. However, it was revealed that the bending stress arising from the housing flange bolt preloads could significantly affect the stress distribution at the strut pilot groove of primary turbine drain passage in the HPOTP housing. Consequently, the information obtained from the present 3-D analysis results should be useful in guiding the development of the SSME HPOTP.

## 1.0 INTRODUCTION

The durability of the SSME system is strongly affected by the severe operating environment. The drain passage in the HPOTP housing flange is one of the critical structural components in the SSME under a variety of environments. The details of the HPOTP system will not be presented here (fig. 1); however, the essentials of the HPOTP drain passage system will be recapitulated for convenience (figs. 2 and 3). The HPOTP raises the pressure of the liquid oxygen to the main injector and preburner injectors to ensure positive injection of oxidizer at all thrust levels. Because the HPOTP is pumping liquid oxygen and is powered by hot, hydrogen-rich gas, extensive shaft seals are needed between the pump and its turbine. The cavity between the primary turbine seal and the secondary turbine seal is drained; the cavity between the secondary turbine seal and the intermediate seal is drained; and the cavity between the intermediate seal and the pump seal is drained, as shown in figures 4, 5, and 6. In addition, the cavity between the two elements of the intermediate seal is purged before, during, and after engine operation. The purge flow splits to set up two pressure barriers; leakage through the intermediate seal gaps and drain line leakages from the above mentioned cavities [1].

In these drain systems, fillet locations between drain holes and the hot gas manifold seal pilot groove in the HPOTP main mounting flange have historically experienced circumferential surface cracks in various locations. It has been believed that these cracks are due to local yielding in compression during the HPOTP installation into the SSME engine powerhead. Upon pump

removal from the powerhead and the relaxation of the installation preloads, the residual strain field in these regions changes to tension and reaches magnitudes sufficient for cracking to initiate by low cycle fatigue (LCF). Note that the cracked region of the HPOTP housing flange is indicated in figure 7. Previously, this subject was studied with the axisymmetric finite element models [2]. However, since the actual hardware of the HPOTP housing has highly nonsymmetric geometry, the analysis models should clearly identify such items as geometry, applied loads, material types, and other input references. Thus, taking into account such items, the initial effort was to create a 3-D finite element model. The analysis was then performed with this model using an individual loading and combined loadings including the thermal loads. Finally, the detailed stresses and deflections of the SSME HPOTP housing were obtained from these analyses.

In summary, the purpose of this study was to obtain the detailed stresses from a 3-D finite element model of the SSME HPOTP housing and to see an influence of the housing flange bolt preloads on the stress fields at the housing flange fillet areas.

## 2.0 MODEL DESCRIPTION

A 3-D finite element ANSYS model of the HPOTP housing was constructed using eight-node isoparametric elements by Lockheed [3]. However, since the Lockheed pump housing model does not have housing flange bolt holes on the housing flange, the ANSYS model was revised to include the flange bolt holes using the Intergraph system [4] and ANSYS [5]. In the revised model, isoparametric hexhedron and solid wedge elements were also used like the Lockheed model. The final model has 3,703 elements with 4,793 nodes. The detailed components of the model are shown in figure 7 for the primary turbine drain system. For the presentation of analysis results, locations of the pump housing drain system exit holes are identified in figure 8. Sections AA ($\theta = 26°$) and CC ($\theta = 146°$) represent the primary turbine drain exit holes. Section DD ($\theta = 86°$ and 166°) represent the secondary turbine drain, and sections BB and NN ($\theta = -14°$, $-74°$, and $-114°$) represent the primary oxidizer drain. The locations of radial drain holes and manifolds of the primary turbine, secondary turbine, and primary oxidizer drains are identified in the cross-sectional view of the HPOTP housing shown in figure 9. The circumferential location of radial holes of the primary turbine, secondary turbine, and primary oxidizer drains is shown in figures 10 through 12, respectively. Cross-sectional views of the primary turbine, secondary turbine, and primary oxidizer drains showing the drain exit and axial holes are presented in figures 13 through 15 with the angle of station $\theta = 26°$, 86°, and $-114°$, respectively. The hidden line plot of a cut-away view of the ANSYS 3-D finite element model of the HPOTP pump housing is shown in figure 16 to show the internal structure. Note that the mixed coolant manifold has not been included in the model of the pump housing.

## 3.0 MODEL LOADING

The scope of this work was to perform detailed environmental stress analyses of the SSME HPOTP housing flange areas at full power level (FPL). Operational conditions of FPL, and the associated environments and loads, were therefore provided by NASA/MSFC, Rocketdyne division

of Rockwell International, and Lockheed Missiles and Space Company for the numerical simulation. In the present analysis, the FPL thermal and pressure loads and housing flange bolt preloads were taken as operational conditions. In this analysis, temperature input was obtained from an ANSYS steady-state thermal analysis performed by Lockheed. The temperatures from the Lockheed analysis were given in reference [3]. Pump housing pressures provided by Rocketdyne are shown in figure 17 and table 1. The TMPINT command of the AUX1 in ANSYS was then used to interface a Lockheed thermal model with the present model. The TMPINT command caused temperatures to be interpolated from the Lockheed model for the current model. As a result of temperature interpolation between two models, the temperature distribution for section CC of the primary turbine is shown in figure 18 with large thermal gradients indicated. The flange bolt preloads (provided by Rocketdyne) were also applied to the current model. There are 30 bolts on the housing flange in the actual HPOTP housing, but 36 bolt holes were used in the current model because it was difficult to introduce 30 bolt holes on the Lockheed model. Ultimate strength of a flange bolt was 72,780 lb, and maximum preload was 69 percent of ultimate strength, which implied that a total preload was equal to 1.5065e6 lb for 30 bolts. Therefore, 1.8078e6 lb for 36 bolts were applied to the current HPOTP housing models. In other words, this means that 5.0217e4 lb per bolt was applied in both models. The pressure loads (obtained from Rocketdyne) were also applied on the pump housing, but the pressures inside the manifold and drain passages of the pump housing were excluded from this analysis as its influence on this analysis was assumed to be negligible (fig. 17).

## 4.0 BOUNDARY CONDITIONS

Displacement boundary conditions for the current HPOTP housing model are shown in figure 19. Considering an operating condition at FPL, prescribed boundary conditions were applied to constrain all nodes in two directions ($x$- and $y$-displacements) at the base of the model which lie on a plane where the housing is connected to the dual inlet on the pump. Additional boundary conditions were imposed to prevent a flange motion in the $z$-direction.

## 5.0 MATERIAL PROPERTIES

Inconel 718 material property data, obtained from the Rockwell Materials Properties Manual, were used for the present analysis [6]. The material properties of Young's modulus, Poisson's ratio, and the coefficient of thermal expansion for Inconel 718 at a temperature range from 0 °R to 2000 °R are shown in table 3.

## 6.0 RESULTS

The 3-D finite element models served for prediction of stresses in the HPOTP housing flange fillet areas. From the analysis results, it was observed that stresses obtained from the present models were much below a yield stress of Inconel 718 (150 ksi). The results are presented to show

the stress distribution at the HPOTP housing flange fillet areas under the various loading conditions. It is noted that the stresses in this study are computed by averaging the nodal stress components and combined stresses of the node being processed for all elements that are connected to that node [5]. The stress components for the primary turbine drain, secondary turbine drain, primary oxidizer drain, and secondary oxidizer drain under a preload case are listed in table 2. However, an equivalent stress based on von Mises yield criterion has been chosen for the purpose of comparison with each loading case. This equivalent stress is used to compare a multiaxial stress state with the minimum guaranteed uniaxial material properties. In this study, the effective stress contours on section CC along the primary turbine drain passage line are made in figures. A deformed shape for section CC ($\theta = 146°$) of the primary turbine drain passage line is also made in figures. In the displacement figures, the dashed line represents an undeformed geometry.

## 6.1 Analysis Model Under Housing Flange Bolt Preloads

Under this loading condition, a deformed geometry for section CC ($\theta = 146°$) of the primary turbine drain passage is shown in figure 21. The stress contour on the same section of the primary turbine drain passage is presented in figure 20. From this analysis, it was found that a large bending occurred in the upper flange as shown in figures 20 and 21. In figure 21, the stress values ranging from 36,265 psi to 54,020 psi of an equivalent stress at the flange fillet area, where the cracks have occurred, were observed. No stresses as high as the Inconel 718 yield stress (150 ksi) were shown at this region.

## 6.2 Analysis Model Under Pressure Loads

In figure 22, considerable deformations have been observed at the primary oxidizer manifold, axial drain hole, and primary turbine manifold areas. The stress contour presented in figure 23 shows a stress of 4,387 psi at the flange strut fillet region. As can be seen, no high stresses have been found at the flange crack area.

## 6.3 Analysis Model Under Thermal Loads

Figure 24 shows a considerable deformation at the primary turbine manifold but small deformations at the fillet region. However, an overall expansion in the drain passage section has been observed under this loading case. In figure 25, it has been observed that the ski slope area is highly stressed by ranging from 85,196 psi to 101,606 psi. However, at the flange fillet section, a stress of 35,965 psi has been observed. The temperature distribution in section CC is presented in figure 18. Compared to the other sections, higher stresses were observed in sections CC and AA.

## 6.4 Analysis Model Under Flange Bolt Preload Plus Pressure Load

In this loading condition compared to the pressure loading case of section 6.2, a displacement direction change was observed at the upper flange, and as can be seen in figure 26 a small deformation occurred in general except in the upper flange area. In figure 27, stresses ranging from 36,492 psi to 53,876 psi at the flange fillet were observed.

## 6.5 Analysis Model Under Flange Bolt Preload Plus Thermal Load

As seen in figure 28, no significant deformation has been indicated at the flange fillet area under this loading case even though a considerable deformation has been observed in an individual loading case due to thermal load and preload. Figure 29 shows an equivalent stress ranging from 42,446 psi to 61,797 psi at a thin flange section.

## 6.6 Analysis Model Under Thermal Load Plus Pressure Load

This simulation case has been taken as an operational loading condition neglecting an effect of the housing flange bolt preloads. This loading case produced 24,075 psi at the flange fillet. Also as indicated in figure 30, section CC was confirmed in the highest stressed region even though the flange preloads were ignored. In figure 31, the significant deformations have also been observed in the primary turbine manifold and drain exit hole regions.

## 6.7 Analysis Model Under Flange Bolt Preload Plus Thermal Load Plus Pressure Load

This final load case has been taken to determine the effect of preloads on the flange in the main pump housing under actual operational condition at FPL. As indicated in figure 32, compared with the case of section 6.6, more flange bending has occurred. A stress of 49,440 psi has been observed at the flange fillet in figure 33. Compared to the case of section 6.6, this case produced more than 200-percent increase in stress at the flange fillet. From this comparison, it was determined that the flange bolt preload yielded significantly different results under actual operational condition of FPL even though there appeared to be a fairly low stress at the flange fillet section with respect to the Inconel 718 yield stress (150 ksi).

# 7.0 CONCLUSIONS AND DISCUSSIONS

The SSME HPOTP contains several components that are highly stressed. In the present analysis, the HPOTP housing has been of particular concern because of the detection of cracks on the flange fillets in the housing. Whether these cracks occur as a result of fatigue stresses due to the engine installation process or from residual stresses due to the manufacturing process, they must be repaired. The present analysis reveals that an effect of the flange bolt preloads in the HPOTP main housing can be very significant in stress distribution at the sharp flange fillet section on primary turbine drain passage lines of the HPOTP main housing. In addition to this revelation, a fairly comfortable margin of stresses at the flange fillet with respect to the yield stress of Inconel 718 is shown in this analysis. However, since it has been believed that the HPOTP housing flange cracks are due to local yielding during the HPOTP installation into the SSME engine powerhead, the coarseness of finite elements and a simplification of the actual hardware in the present finite element modeling should be further refined in a future analysis.

Table 1. Applied pressure on HPOTP housing model.

| Number in Figure 11 | Description | Pressure (psia) |
|---|---|---|
| 1 | Mixed Coolant Manifold | 5,682.0 |
| 2 | Reflector Cavity | 3,679.0 |
| 3 | Second Stage Turbine Disk Aft Cavity | 3,680.0 |
| 4 | Bearing Support/Cartridge Interface | 548.0 |

Table 2. Stress components of primary turbine drain, secondary turbine drain, primary oxidizer drain, secondary oxidizer drain under flange bolt preload at crack location, unit = psi.

| | SIGE | SIG1 | SIG2 | SIG3 | Sx | Sy | Sz | Sxy | Syz | Sxz |
|---|---|---|---|---|---|---|---|---|---|---|
| AA (θ=26°) | 26,750 ~ 52,930 | -25,390 ~ -7,543 | -43,680 ~ -25,347 | -73,629 | -45,731 ~ -28,050 | -43,672 ~ -24,944 | -61,981 | -534 ~ 323 | -534 ~ 599 | -13,878 |
| DD (θ=86°) | 27,003 ~ 53,110 | -25,417 ~ -7,537 | -43,643 ~ -25,293 | -73,781 | -45,768 ~ -28,080 | -43,633 ~ -24,921 | -62,106 | -512 ~ 303 | -578 ~ 556 | -13,919 |
| CC (θ=146°) | 27,388 ~ 54,020 | -25,771 ~ -7,657 | -44,545 ~ -25,957 | -74,845 | -46,802 ~ -28,773 | -44,598 ~ -25,417 | -62,831 | -760 ~ -167 | -481 ~ 435 | -14,201 |
| DD (θ=166°) | 27,423 ~ 54,090 | -25,736 ~ -7,607 | -44,532 ~ -25,935 | -74,953 | -46,828 ~ -28,793 | -44,597 ~ -25,407 | -62,768 | 183 ~ 762 | -463 ~ 454 | -14,166 |
| NN (θ=216°) | 26,950 ~ 53,073 | -25,426 ~ -7,547 | -43,649 ~ -25,301 | -73,726 | -45,772 ~ -28,084 | -43,639 ~ -24,899 | -62,062 | -673 ~ 693 | -628 ~ 504 | -13,897 |
| NN (θ=286°) | 26,915 ~ 53,012 | -25,390 ~ -7,543 | -43,662 ~ -25,329 | -73,622 | -45,734 ~ -28,051 | -43,654 ~ -24,928 | -61,977 | -507 ~ 326 | -530 ~ 602 | -13,879 |
| BB (θ=346°) | 26,946 ~ 53,066 | -25,425 ~ -7,548 | -43,682 ~ -25,352 | -73,721 | -45,755 ~ -28,067 | -43,672 ~ -24,949 | -62,064 | -533 ~ 300 | -626 ~ 506 | -13,896 |

Table 3. Temperature dependent material properties.

| temp / mat'ls | 0 °R | 400 °R | 800 °R | 1200 °R | 1600 °R | 2000 °R |
|---|---|---|---|---|---|---|
| E (psia) | 3.01e7 | 2.98e7 | 2.9e7 | 2.7e7 | 2.45e7 | 2.15e7 |
| $\nu$ | 0.22 | 0.285 | 0.29 | 0.28 | 0.29 | 0.37 |
| $\alpha$ (in/in/° R) | 5.2e-6 | 6.9e-6 | 7.6e-6 | 8.0e-6 | 8.45e-6 | 9.45e-6 |

Figure 1. SSME powerhead.

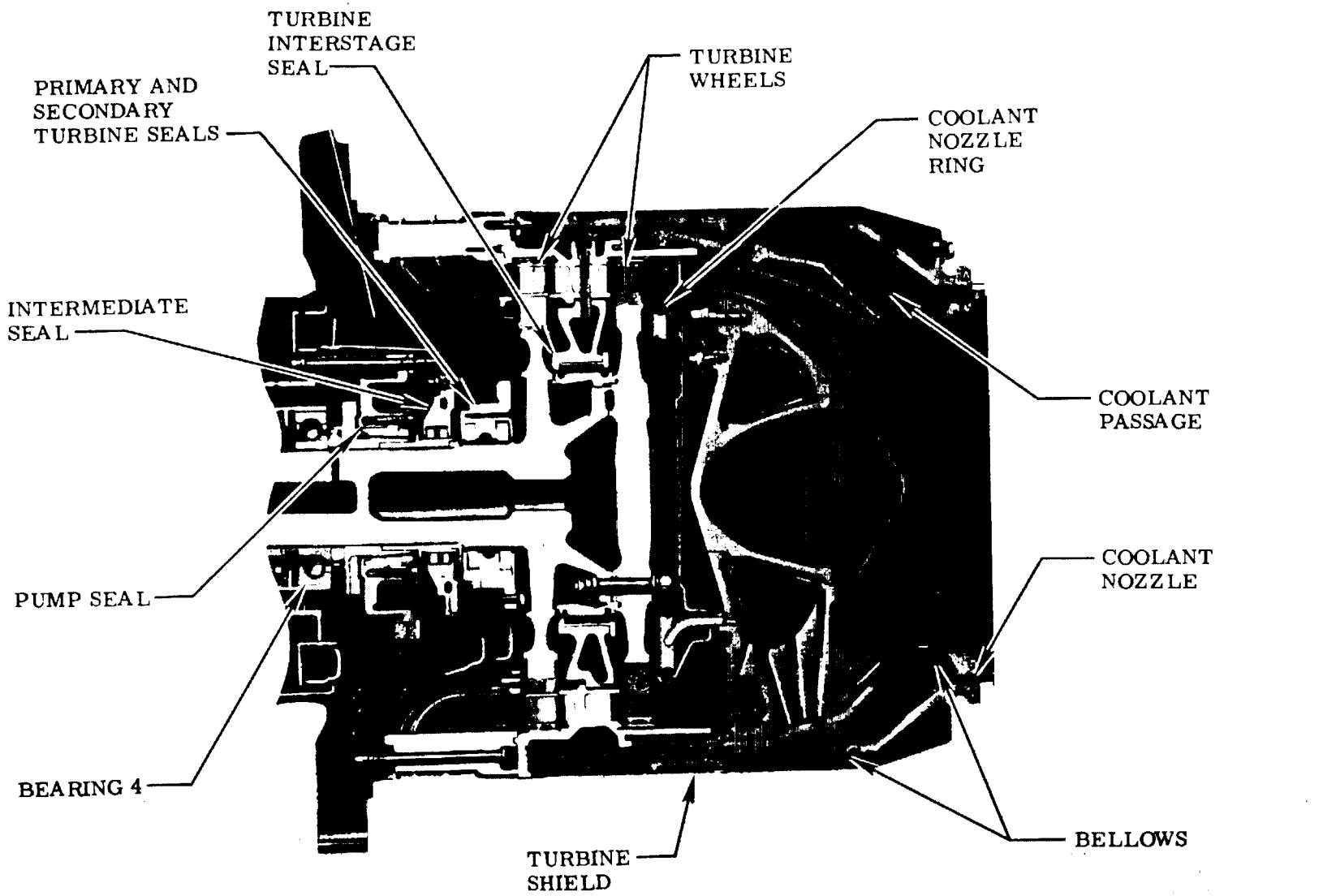


Figure 2. HPOTP turbine section.

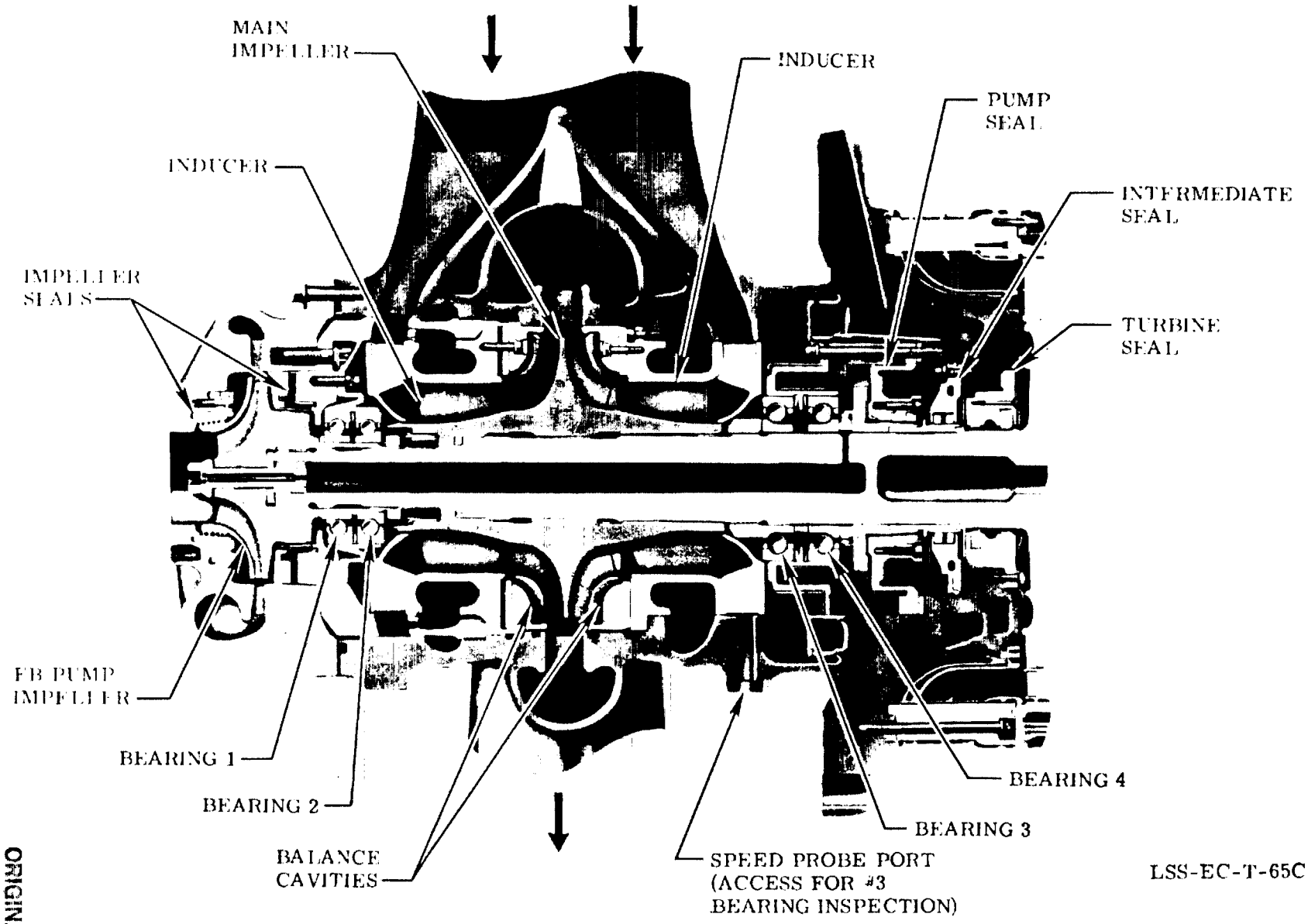


Figure 3. HPOTP pump section.

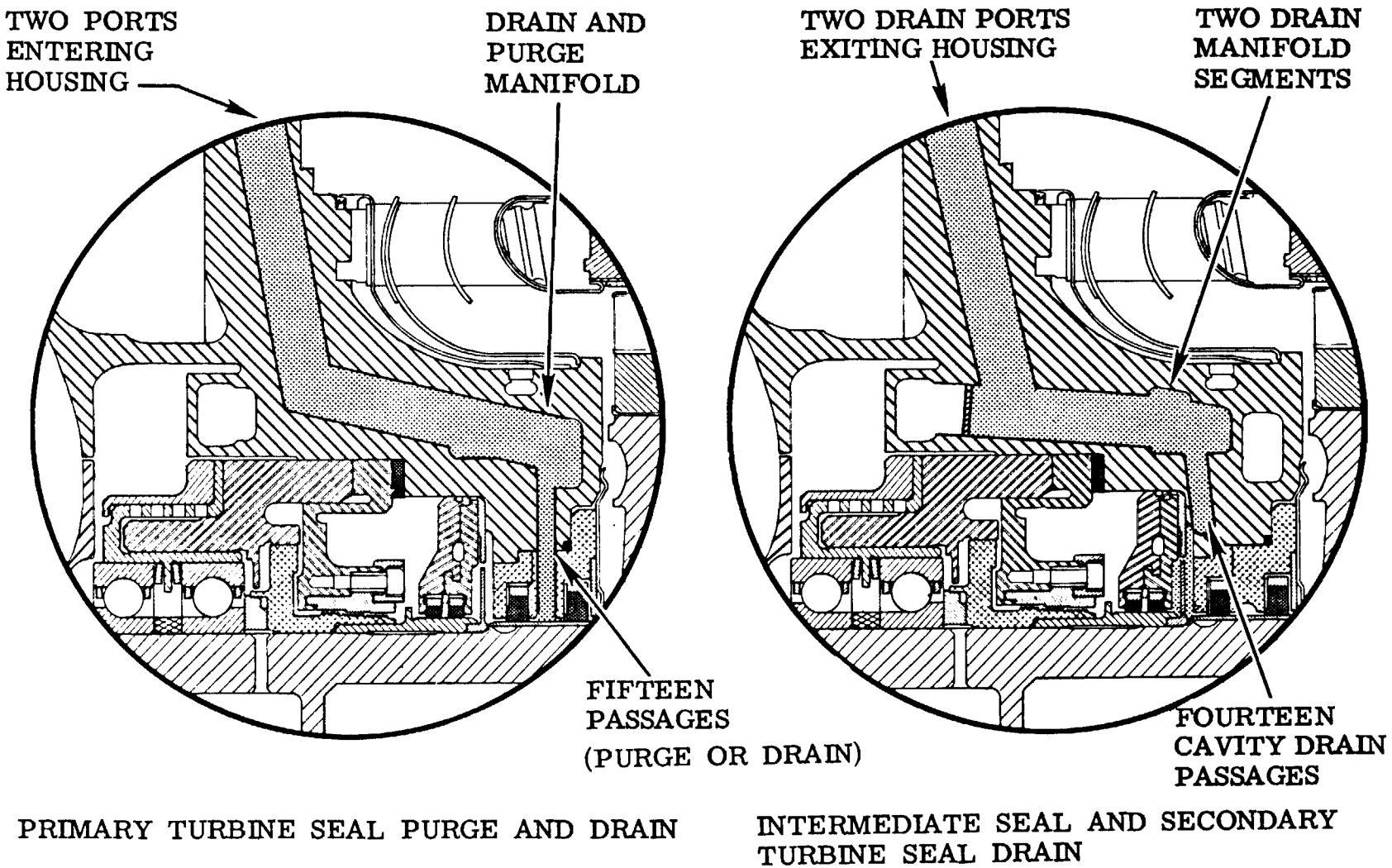


Figure 4. HPOTP purge and drain details (1).

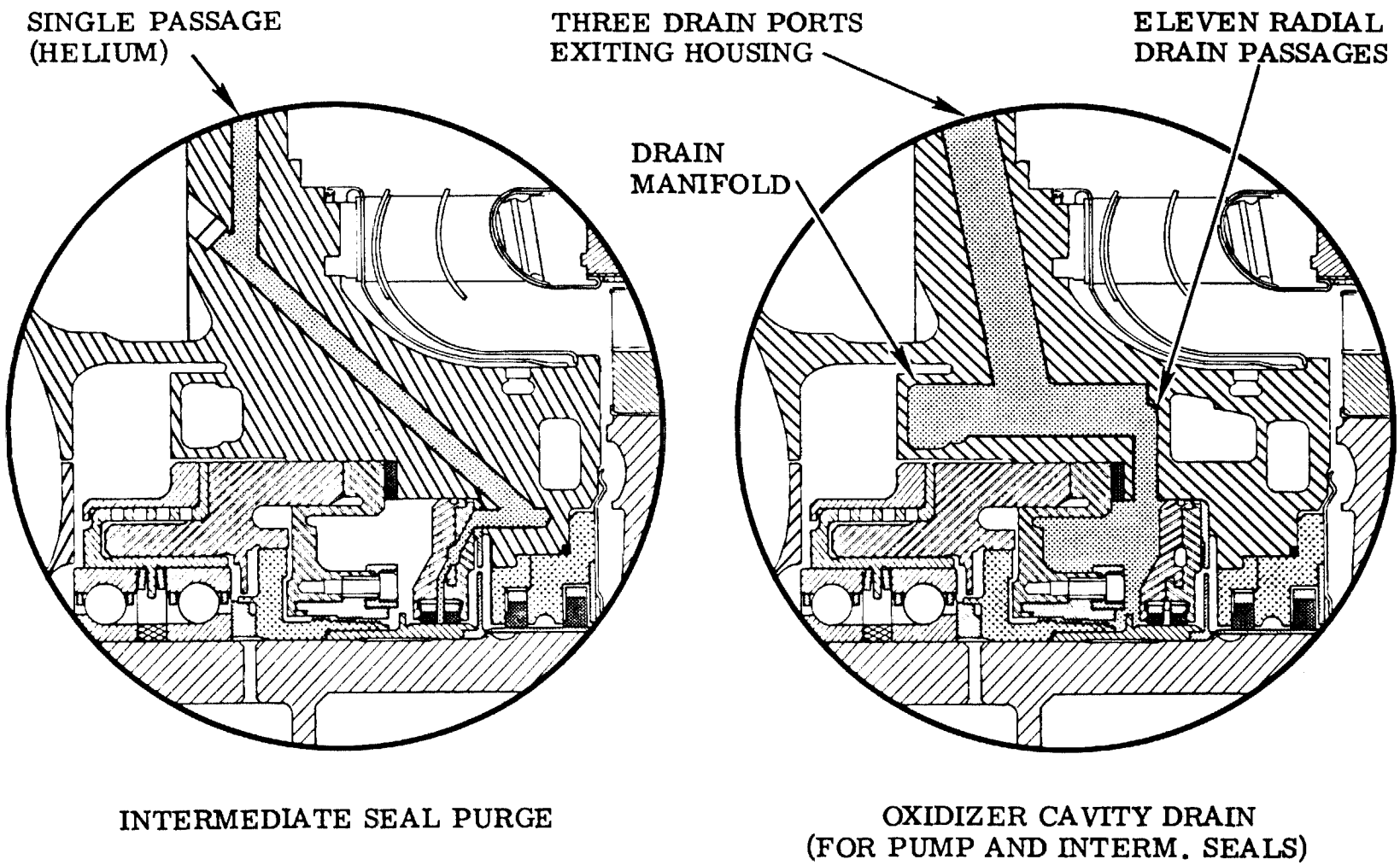


Figure 5. HPOTP purge and drain details (2).

(ENGINES 2004 AND SUBSEQUENT)

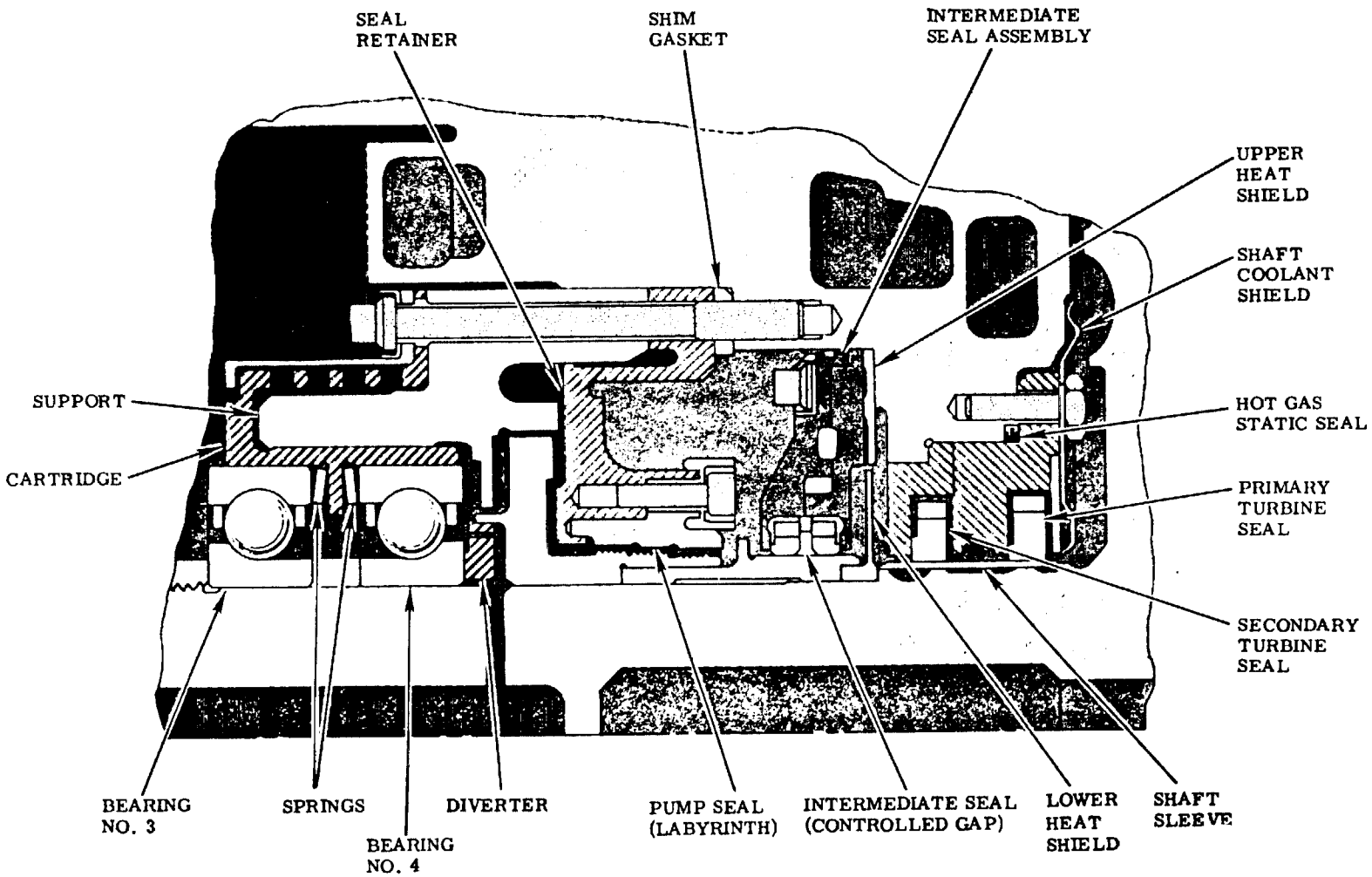


Figure 6. HPOTP seal group.

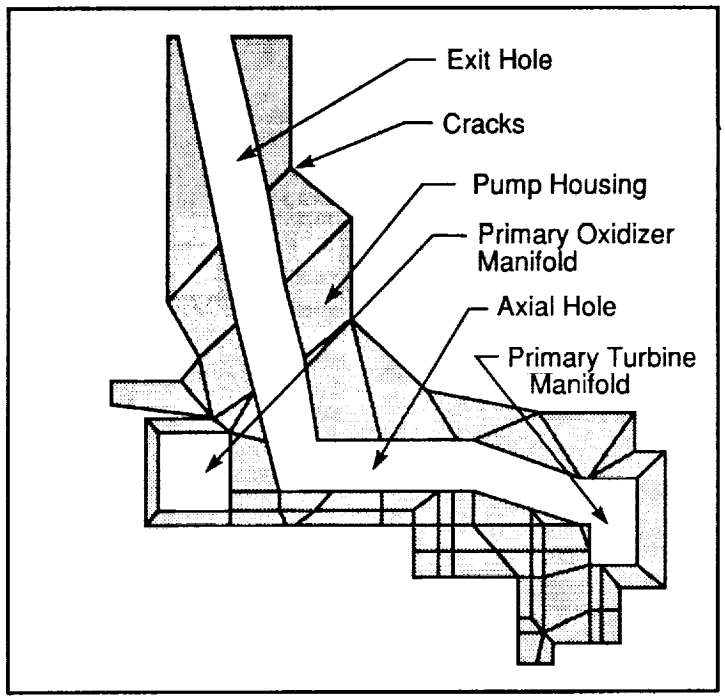


Figure 7. Components of HPOTP housing model and location of cracks.

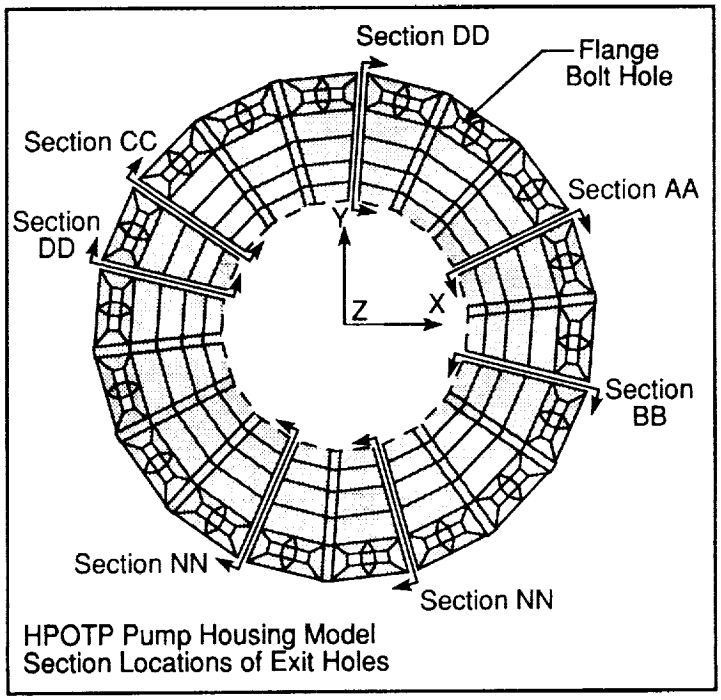


Figure 8. Locations of drain passage of HPOTP housing.

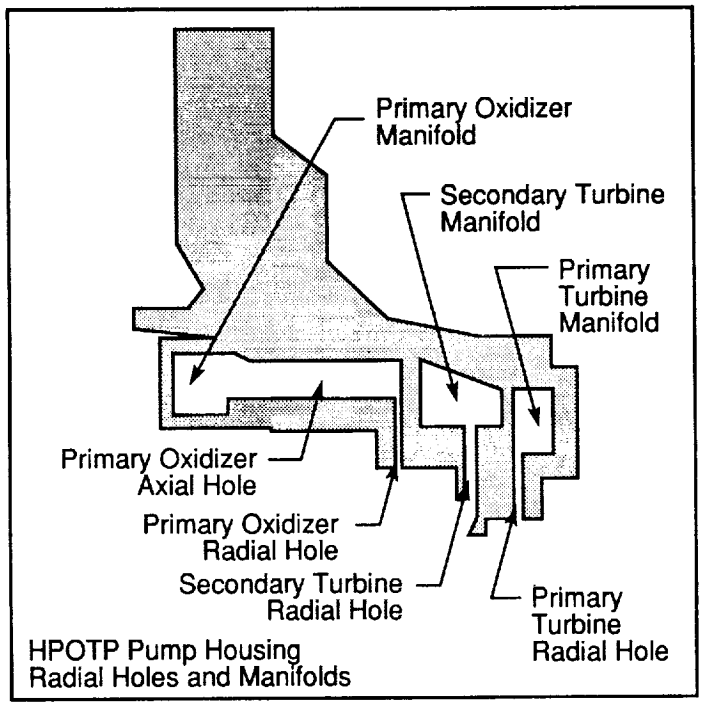


Figure 9. Radial holes and manifolds of HPOTP housing.

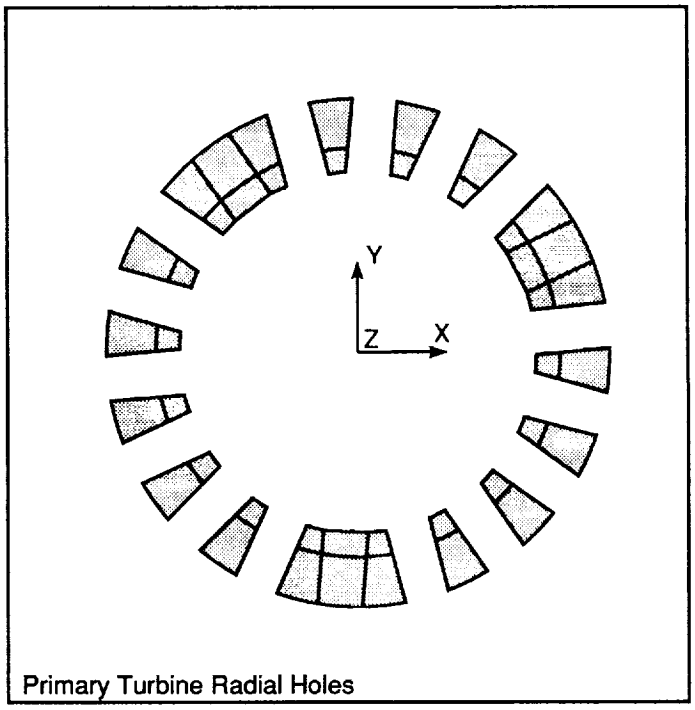


Figure 10. Locations of turbine radial holes in HPOTP.

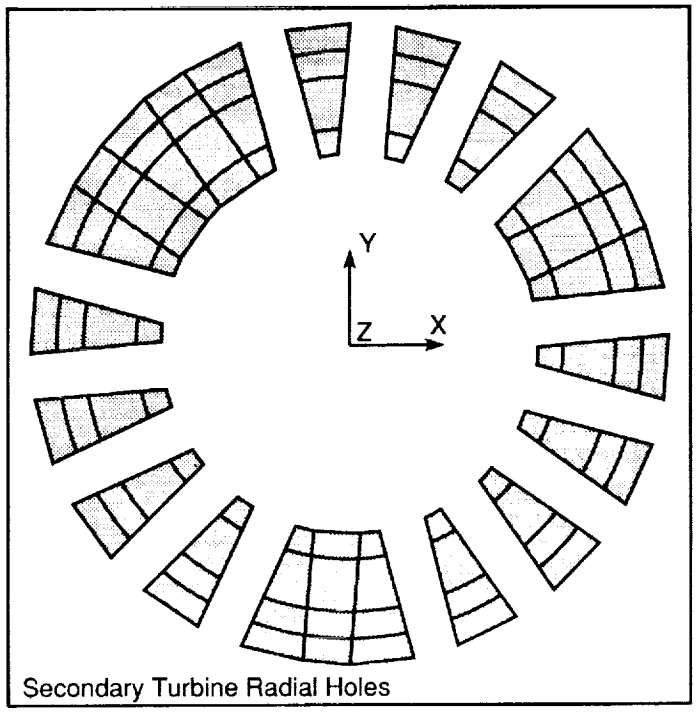


Figure 11. Locations of secondary turbine radial holes.

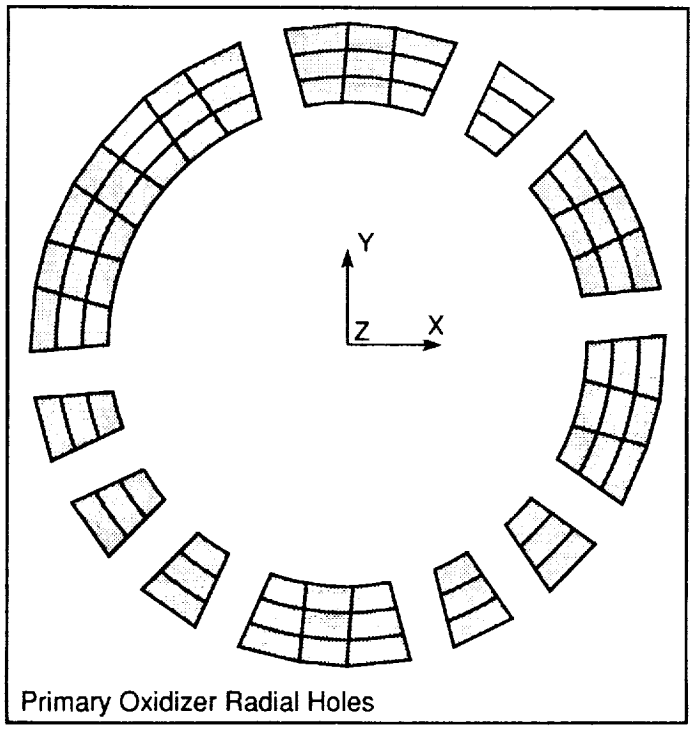


Figure 12. Locations of primary oxidizer radial holes.

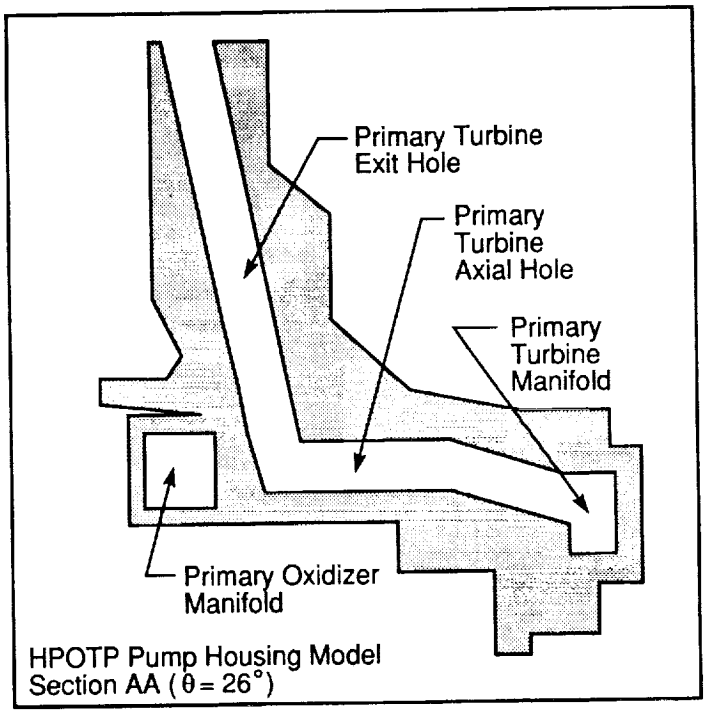


Figure 13. Section AA of HPOTP housing.

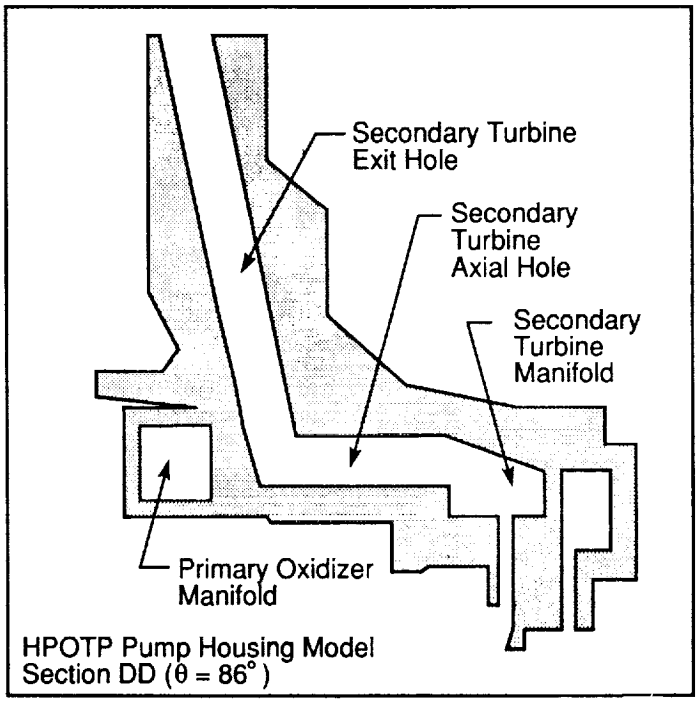


Figure 14. Section DD of HPOTP housing.

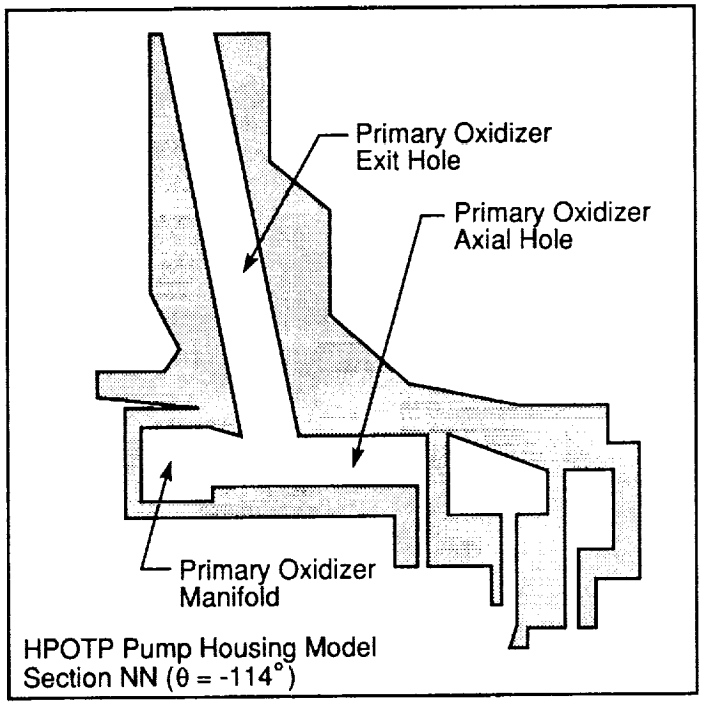


Figure 15. Section NN of HPOTP housing.

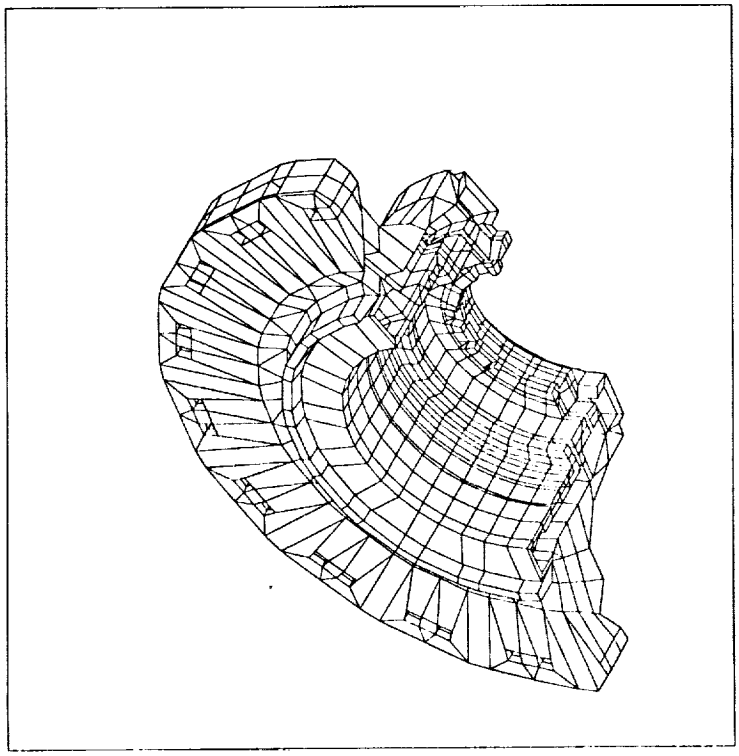

Figure 16. Cutaway view of HPOTP housing from pump toward to turbine end.

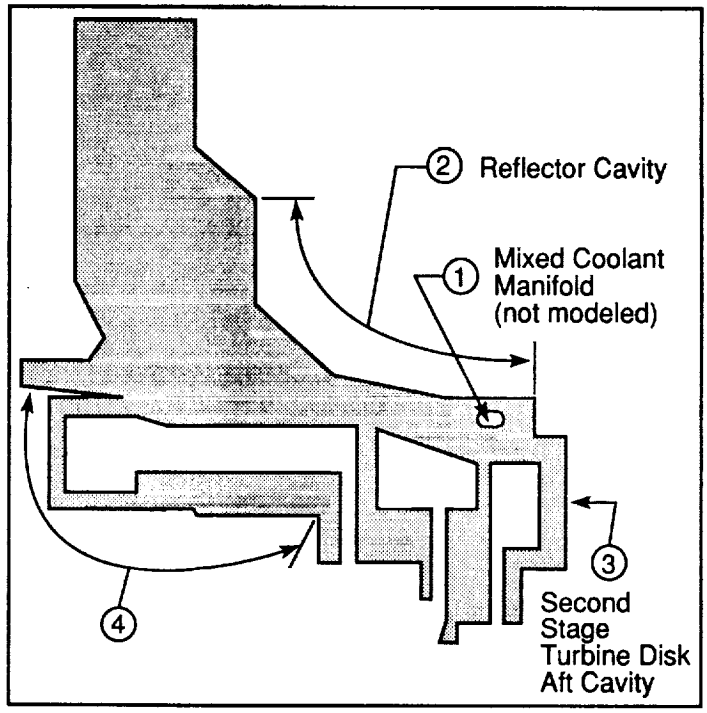


Figure 17. Locations of pressurized surfaces in HPOTP housing model.

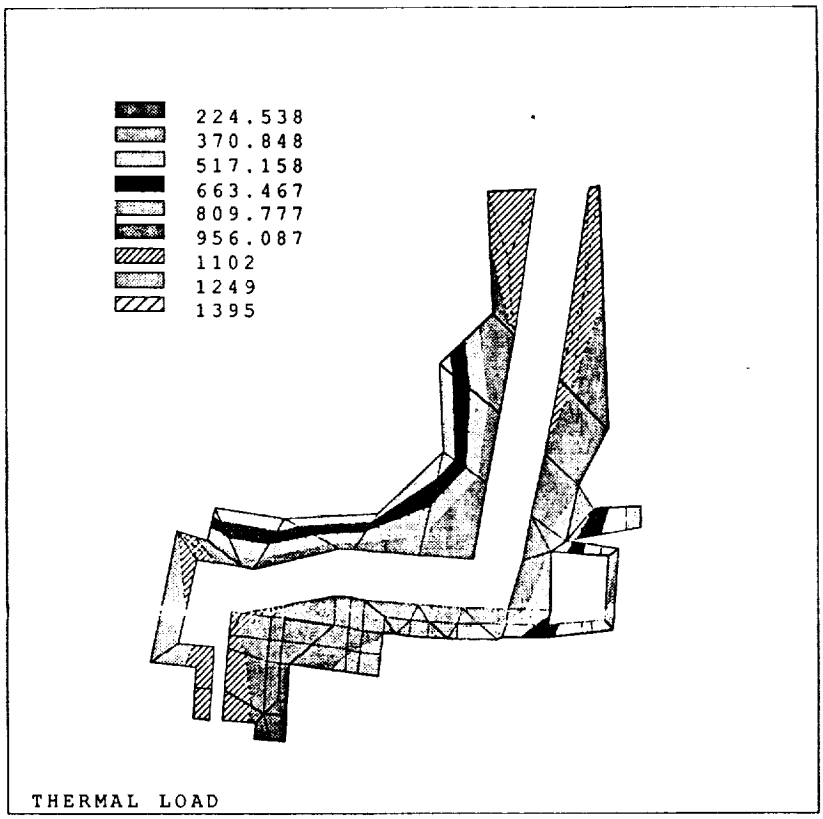


Figure 18. Temperature distributions of section CC.

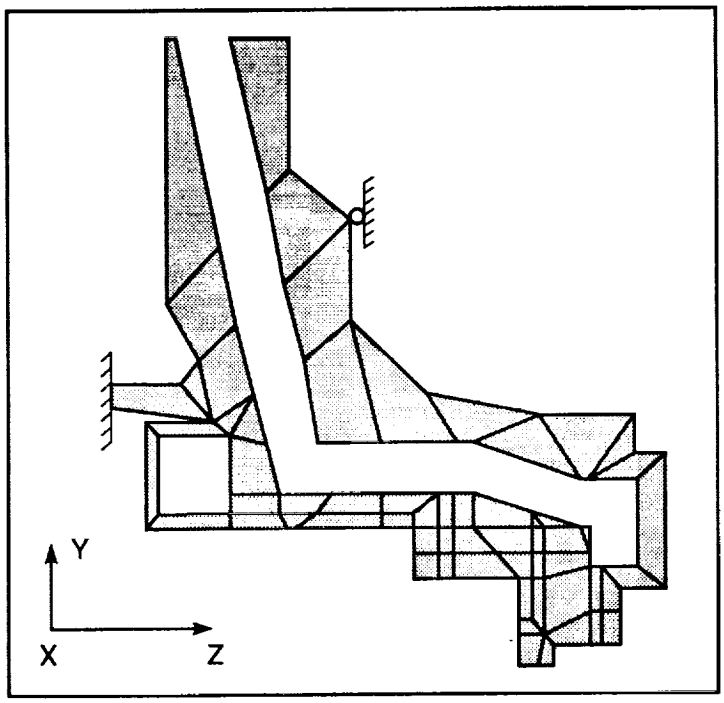


Figure 19. Coordinate systems and boundary conditions used in HPOTP housing analysis models.

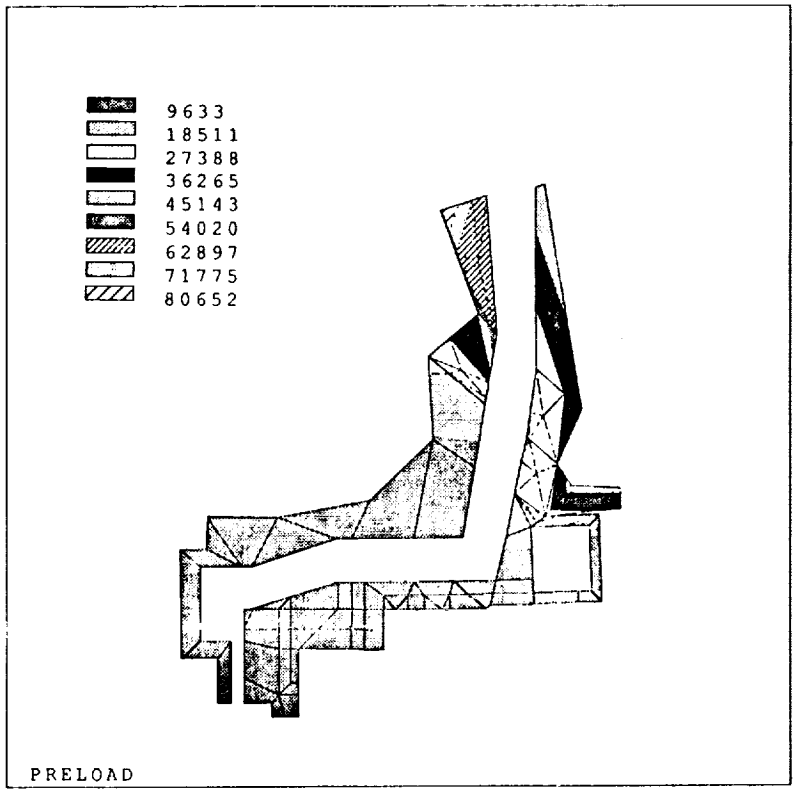


Figure 20. Stress distribution of flange bolt preload at section CC.

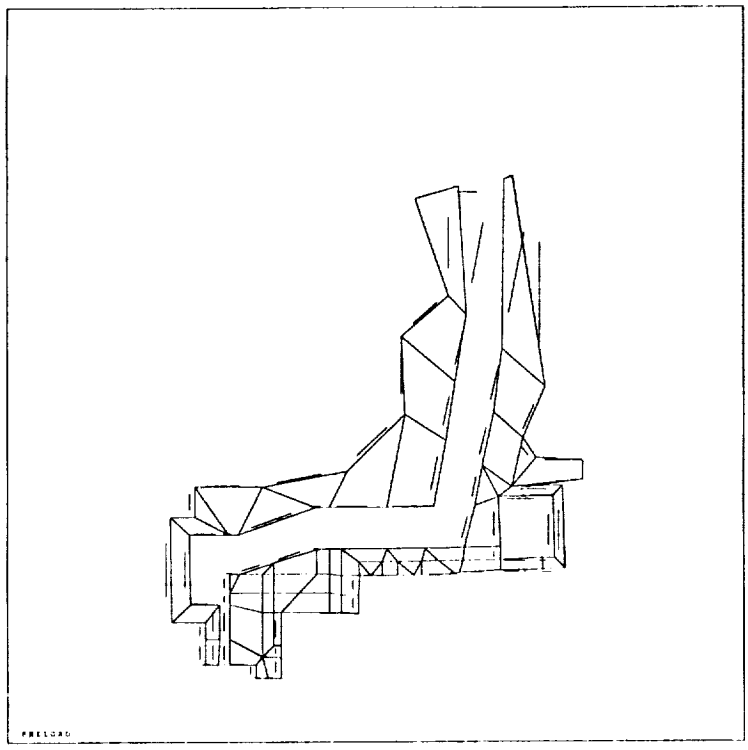

Figure 21. Deformation of section CC on undeformed section under flange bolt preload.

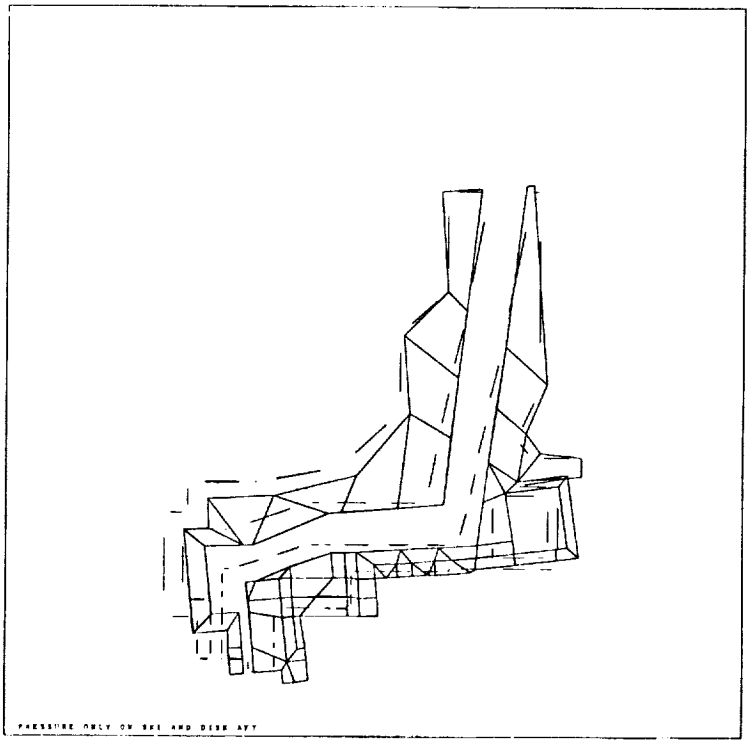

Figure 22. Deformation of section CC on undeformed section under applied pressure loading.

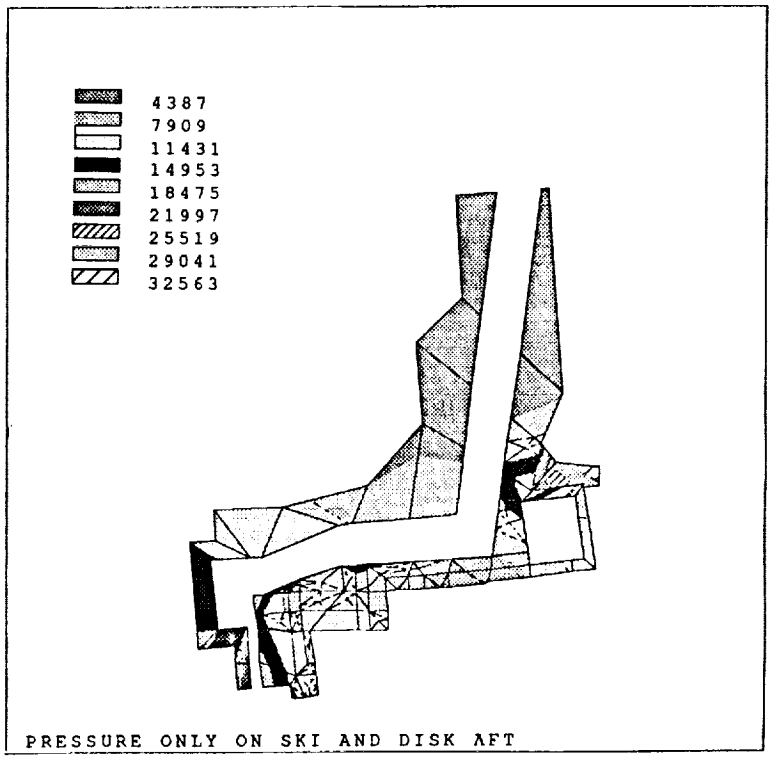


Figure 23. Stress distribution of section CC under applied pressure loading.

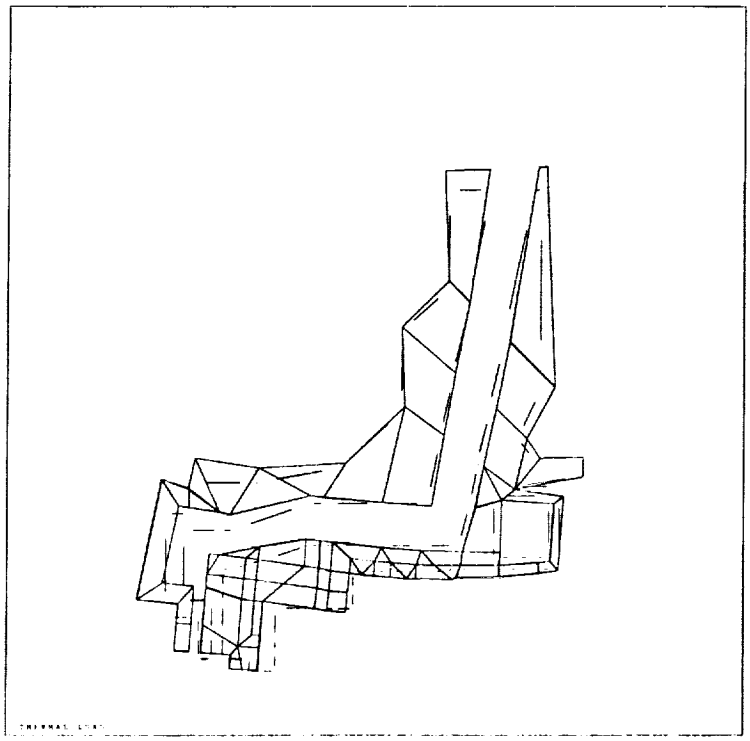

Figure 24. Deformation of section CC on undeformed section under thermal load.

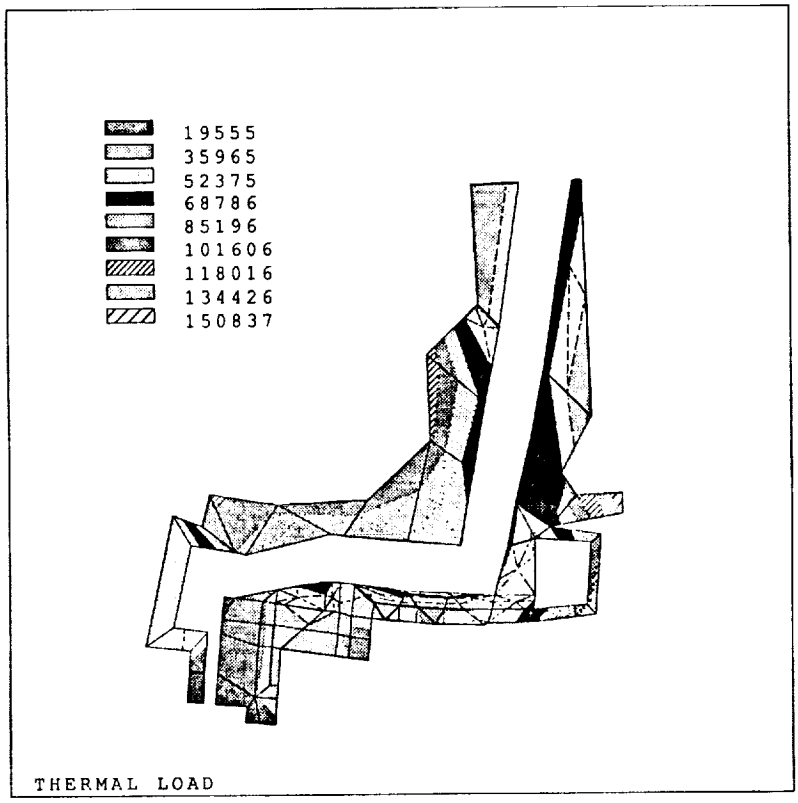


Figure 25. Stress distribution of section CC under thermal loading.

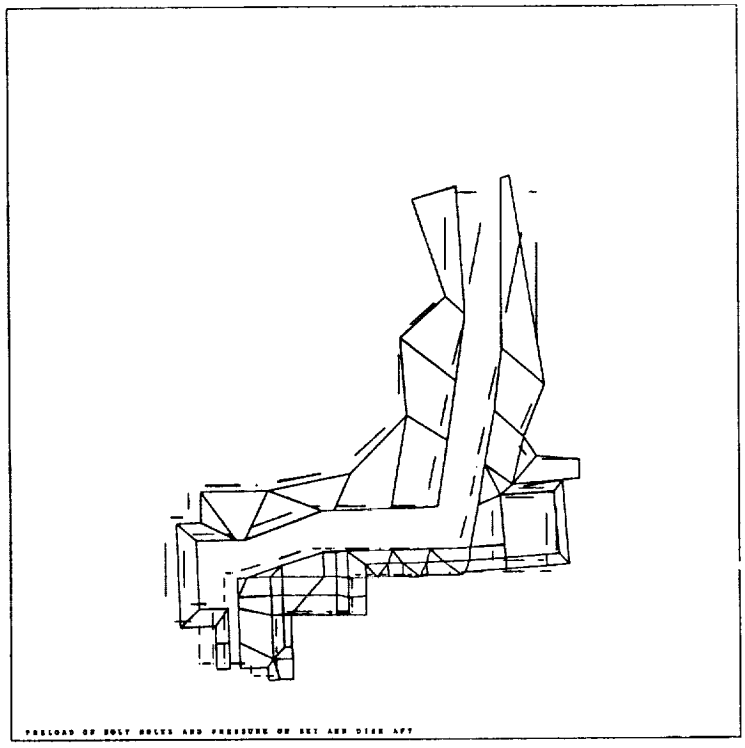

Figure 26. Deformation of section CC on undeformed section under flange bolt preload plus applied pressure load.

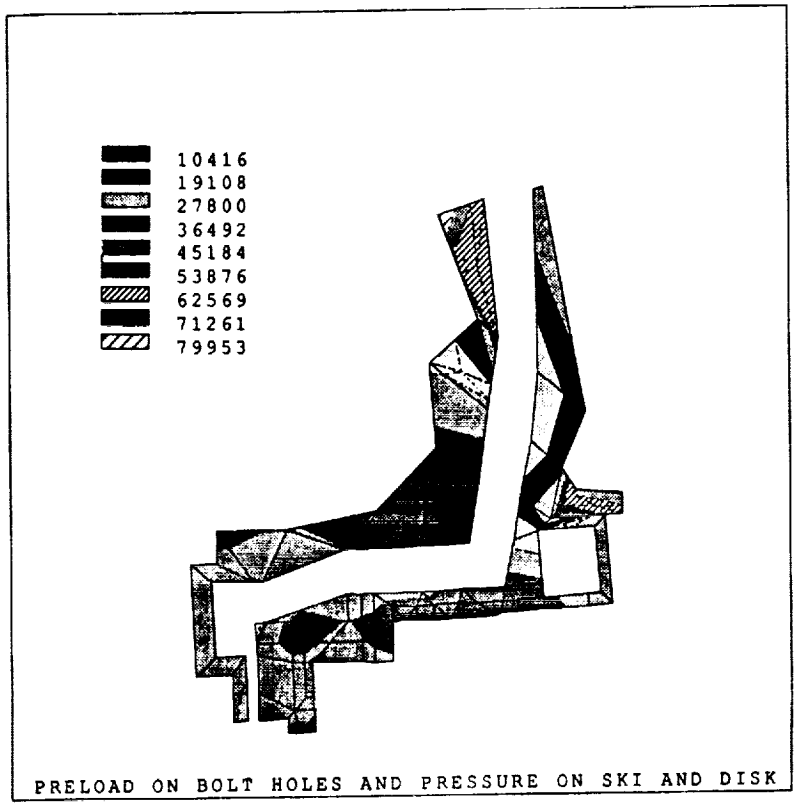


Figure 27. Stress distribution of section CC under flange bolt preload plus applied pressure load.

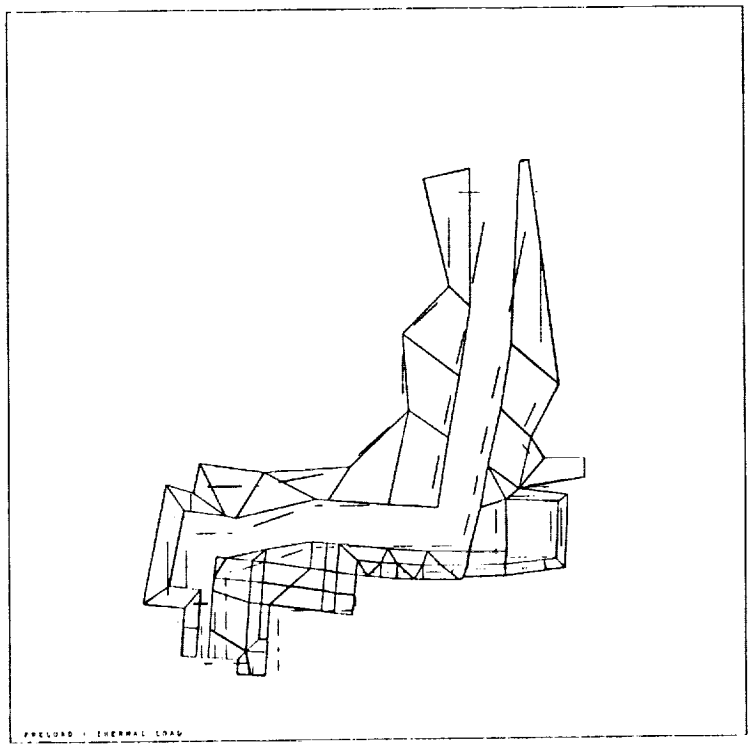

Figure 28. Deformation of section CC on undeformed section under flange bolt preload plus thermal load.


Figure 29. Stress distribution of section CC under flange bolt preload plus thermal load.

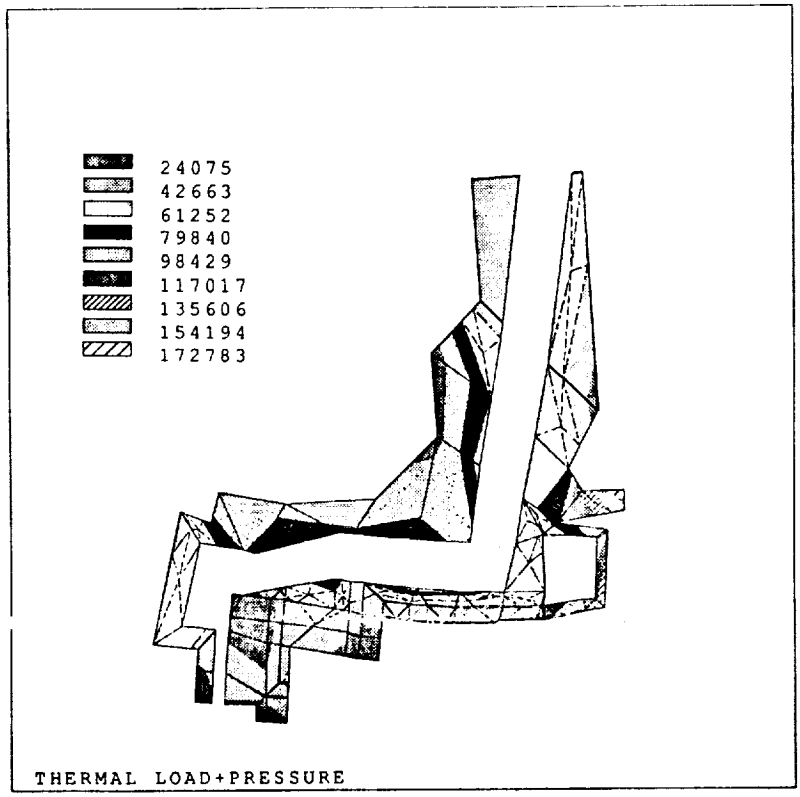


Figure 30. Stress distribution of section CC under applied pressure plus thermal load

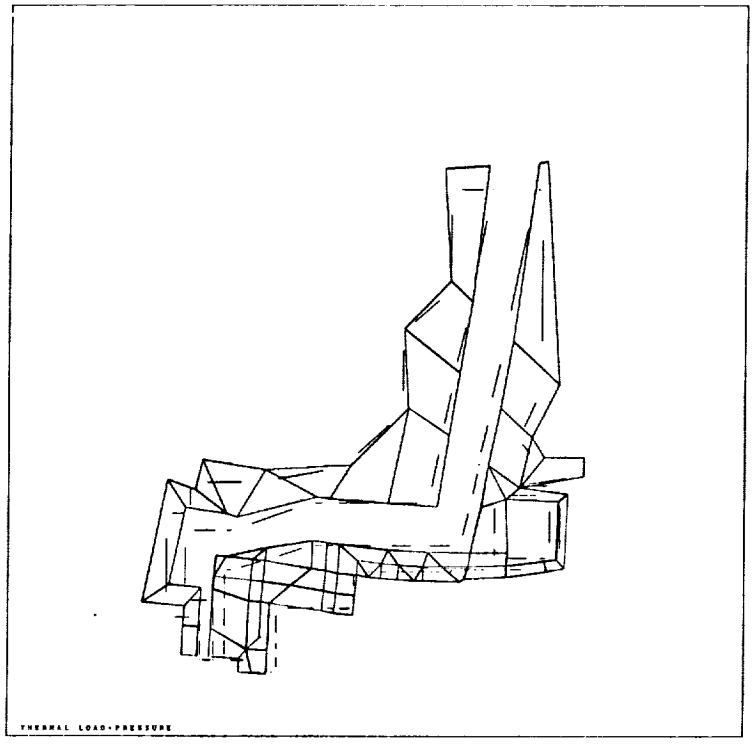

Figure 31. Deformation of section CC on undeformed section under applied pressure plus thermal load.

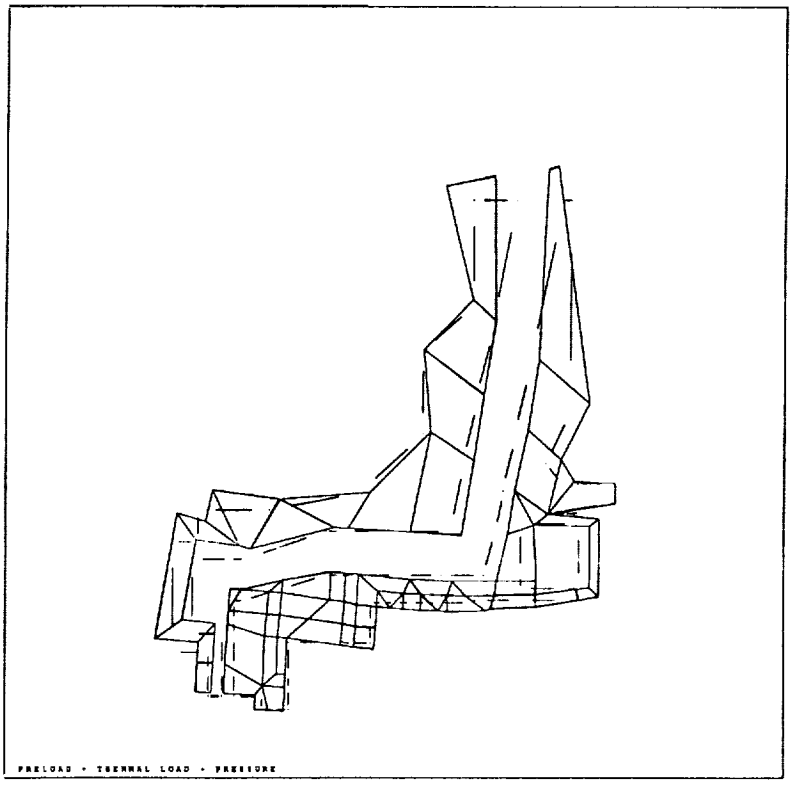

Figure 32. Deformation of section CC on undeformed section under applied pressure plus thermal load plus flange bolt preload.


Figure 33. Stress distribution of section CC under applied pressure plus thermal load plus flange bolt preload.

## REFERENCES


1. SSME Orientation (Part A-Engine), Rockwell International Corporation, Rocketdyne Division 02602, August 1, 1988.

2. Private Communication Note, Rocketdyne Division, Rockwell International, 1990.

3. Lockheed Final Report of HPOTP Turbine End Bearing Analysis, LMSC-HEC TR F268584-II, 1989.

4. Intergraph/Finite Element Modeling (I/FEM), DMEC03210, December 15, 1988.

5. ANSYS4.4 User's Manual, Volume I & II, May 1, 1989.

6. Rocketdyne's Materials Properties Manual, Pub. No. 572K, January 31, 1987.

## APPROVAL

## EFFECT OF FLANGE BOLT PRELOAD ON SPACE SHUTTLE MAIN ENGINE HIGH PRESSURE OXIDIZER TURBOPUMP HOUSING ANALYSIS

By J.B. Min, L.M. Johnston, and B. Czekalski

The information in this report has been reviewed for technical content. Review of any information concerning Department of Defensr or nuclear energy activities or programs has been made by the MSFC Security Classification Officer. This report, in its entirety, has been determined to be unclassified.

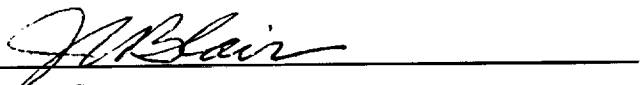

JAMES C. BLAIR
Director, Structures and Dynamics Laboratory

☆U. S. GOVERNMENT PRINTING OFFICE 1991 — 531-081/40059